

# PREPARATION OF UNIAIAL CHART FOR RECTANGULAR CONCRETE-FILLED STEEL COLUMNS BASED ON RIGID PLASTIC PRINCIPLES

Erimiyas Ketema and Shifferaw Taye  
Department of Civil Engineering  
Addis Ababa University

## ABSTRACT

Composite columns are in an increased usage for construction of high-rise and medium-rise buildings, bridges and other structures. However, their design procedure as proposed by the relevant Ethiopian Building Code Standard, which is also a derivative of the corresponding European Standard Eurocode 4, calls for extensive numerical effort for drawing the moment-axial-force interaction charts. Furthermore, the results obtained following those procedures are based on curve-fitting techniques making use of widely sparse control points and, consequently, they produce approximate results. This paper explores the shortcomings of the relevant local building code standard for the design process and presents improved design chart procedures for concrete-filled rectangular steel tube columns. The proposed procedure simplifies the design process and, at the same time, considerably increases the accuracy of results.

A unified approach has been presented for the procedure of establishing interaction design charts for concrete-filled steel tubes (CFTs) under uniaxial bending and valuable charts have been prepared for most frequently encountered shapes in practice – rectangular and square shapes. The proposed procedure may also be developed and adapted to facilitate the preparation of similar design charts for other shapes and material types.

Finally, numerical examples will be presented to demonstrate implementation of the proposed procedure and to provide insight into comparative quality of the charts with those generated according to the relevant national code standard.

## INTRODUCTION

Steel-concrete composite structural elements lie between steel-only and concrete-only system and they constitute a class of structures in which steel and concrete act together compositely. It is the most important and most frequently encountered combination of construction materials with

applications in multi-storey residential and commercial buildings, factories and in a variety of large-span building structures as well as in bridges.

Composite steel-concrete columns can assume a variety of shapes and compositions depending on, among other things, the loading types and relative magnitudes of those loads to which they are subjected. Typical cross sections of such columns are shown in Fig. 1.

The interest in composite construction also develops from the fact that structural and material properties of both steel and concrete are fully

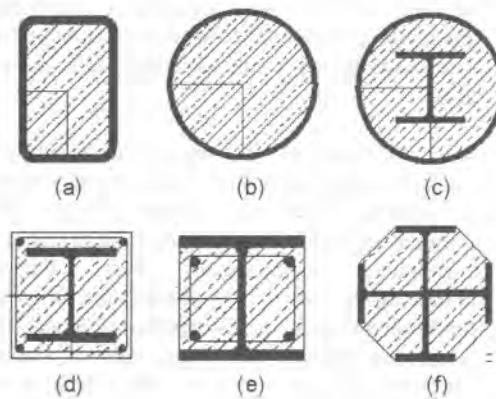


Figure 1 Typical cross-sections of steel-concrete composite columns

utilized in the CFTs. It makes use of attractive features of both materials while it extremely minimizes their undesirable features and properties. These features of composite structural elements are both of structural and non-structural nature. With respect to their structural properties, these essentially different materials are compatible and complementary to each other in that they exhibit an ideal combination of strengths with the concrete efficient in compression and the steel in tension. Furthermore, concrete can restrain slender steel sections from local or lateral-torsional buckling; consequently, strength, stiffness and ductility of the structures constructed from CFTs can be enhanced

simultaneously [2, 3]. With regard to their non-structural behavior, they have almost the same thermal expansion besides the fact that concrete also gives corrosion protection and thermal insulation to the steel at elevated temperatures.

Bond develops either from adhesion between concrete and steel or from friction due to normal stress. Since adhesion is active mainly at the early stage of loading, it is assumed that bond between the concrete and the steel is mainly contributed by friction. Friction develops between the concrete core and the steel tube due to the coefficient of friction and normal contact pressure, which is caused by lateral expansion of the concrete core when subjected to compressive loading. The magnitude of the friction force developed in CFT columns depends on the rigidity of the tube walls against pressure perpendicular to their plane. If the bond is not sufficient to transfer the load between the steel and concrete, it is necessary to provide the top region of the steel tube with mechanical shear connectors at the inside to ensure full composite action.

Since the function of longitudinal reinforcement and transverse confinement, independently working in ordinary reinforced concrete, both can be acquired in CFTs directly from the steel tubes, the traditional longitudinal and transverse reinforcement may be eliminated especially when the structural action is not significantly large. It has also been shown that such type of columns maintain sufficient ductility when high strength concrete is used [4].

Further benefits of composite construction are attributed to the structural planning process. In this respect, the concept of composite construction has given engineers ample opportunity to design composite building systems of structural steel and reinforced concrete to produce more efficient structures when compared to designs using either material alone. As in all design undertakings, the economy of resulting structures is of great concern. In this respect, single composite-column elements, although exhibiting high structural quality and load resistance, are also, in many cases, expensive. This is the case particularly for buildings with small column spacing. However, this is offset by the prevailing desire for larger column-free spans in

buildings to facilitate open planning or greater flexibility in layout as well as provision of larger longitudinal span in bridge pier spacing.

Large span and mega-size structures of both horizontal and vertical topology are called upon to sustain a variety of load types with effective use of construction materials and minimal usage of space by the structural components. To meet many of these conflicting conditions and requirements, there is, thus, a growing interest in utilizing CFTs as primary column members.

CFT columns can, thus, effectively replace other commonly used structural columns such as ordinary reinforced concrete, structural steel with reinforced concrete or structural steel alone with superior performance while at the same time reducing materials costs to a minimum especially when both structural and non-structural features are considered in an integrated manner [5]. It is especially useful in multistory buildings where higher strength capacity is required and flexibility of open space is desired for a maximum range of applications.

There are generally four major topological cross-section layouts of CFTs columns as shown in Fig. 2 depending on the relative magnitude of moment / axial-force combination to which the element is subjected. In general, larger concentration of the steel component is desirable to resist mainly axial-load systems while distributed placement of the steel component is required in cases where the dominance of the flexural moment is significant.

Design of composite columns, as in all types of compression members, calls for a procedural approach in which the effects of both axial and flexural stresses are taken into consideration in order to assess the capabilities of the particular member. To this effect, interaction equations and / or diagrams have been proposed for a variety of structural column systems – steel (see, for example [1]) and concrete (see, for example [6]) under various loading conditions including procedures to produce such diagrams for steel-concrete composite columns [7, 8, 9].

axial force $N$	small	large	moderate	moderate
moment $M$	insignificant	insignificant	moderate	large
$e = M/N$	small	small	moderate	large

Figure 2 Possible arrangement of composite rectangular tubular columns with reference to loading

The purpose of this paper is to propose an improved procedure for developing interaction charts that will have dual purpose: (a) for efficient determination of the necessary cross-sectional dimensions and material requirement for a CFT column under a specified set of loads on one hand and (b) evaluation of the capacity of a given cross-section when the size and relevant material properties of each of the composite constituent materials are known in advance. The proposed charts may be used both for short and long columns. Utilization of the proposed charts will be facilitated and generalized for any cross-sectional shape if their development is based on non-dimensional parameters. Towards this goal, the capacity equations to be developed and subsequently used to establish the charts will be made non-dimensional.

The basic procedure to be followed for chart development and some of the interaction charts

produced following the procedure outlined in this work will be given in the later sections.

### COLUMN LOAD CAPACITY

#### Resistance to Axial Compression and Bending

The cross-sectional resistance of a composite column under axial compression and uniaxial bending is given by an M-N (moment-axial force) interaction curve. The interaction curve can be determined point by point by considering different positions of plastic neutral axis in the principal plane under consideration. The concurrent values of moment and axial resistance are then found from the stress blocks. Fig. 4 illustrates this process for four particular positions of the plastic neutral axis corresponding respectively to the points marker A, B, C, D marked in Fig. 3 and each of these points will be discussed hereafter:

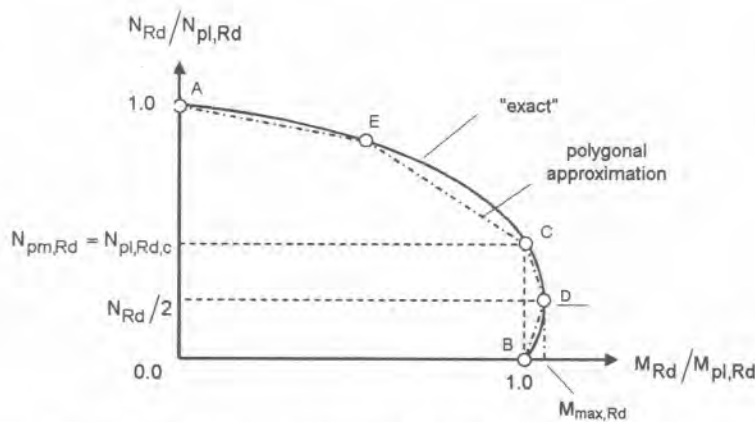


Figure 3 M-N interaction curve for uniaxial bending

- **Point A** : Axial compression resistance alone:

$$N_A = N_{pl,Rd} \quad M_A = 0 \quad (1)$$

- **Point B** : Uniaxial bending resistance alone:

$$N_B = 0 \quad M_B = M_{pl,Rd} \quad (2)$$

- **Point C** : Uniaxial bending resistance identical to that at point *B*, but with a non-zero resultant axial compressive force:

$$N_C = N_{pm,Rd} \quad M_C = M_{pl,Rd} \quad (3)$$

where:  $N_{pm,Rd} = A_c f_{cd}$  is the compressive resistance of the concrete section

- **Point D** : Maximum moment resistance

$$N_D = 0.5 N_{pm,Rd} = 0.5 A_c f_{cd}$$

$$M_D = W_{ps} f_{yd} + 0.5 W_{pc} f_{cd} \quad (4)$$

in which  $W_{ps}$  and  $W_{pc}$  are the plastic moduli, respectively, of the steel section and the concrete. Point *D* corresponds to the maximum moment resistance  $M_{max,Rd}$  that can be achieved by the section. This is greater than  $M_{pl,Rd}$  because the compressive axial force inhibits tensile cracking of the concrete, thus, enhancing its flexural resistance.

- **Point E** : Situated midway between *A* and *C*.

The enhancement of the resistance at point *E* is a little more than that given by direct linear interpolation between *A* and *C*, and determination of this point can therefore be omitted.

The concurrent values of moment and axial resistance are then found from the stress blocks. Ethiopian Building Code Standard EBCS 4 [7] and the corresponding European Standard Eurocode 4 [8] highlight the procedure for determining the four particular positions *A, B, C, D* of the plastic neutral axis as shown in Fig. 3. It is usual to substitute the linearised version *AECDB* (or the simpler *ACDB*) shown in Fig. 3 for the more exact interaction curve after carrying out the calculations to determine these points. However, the results tend to be approximate since the entire curve is based only on four control points. Thus, this paper presents an improved procedure for the establishment of more refined moment – axial-force interaction curves.

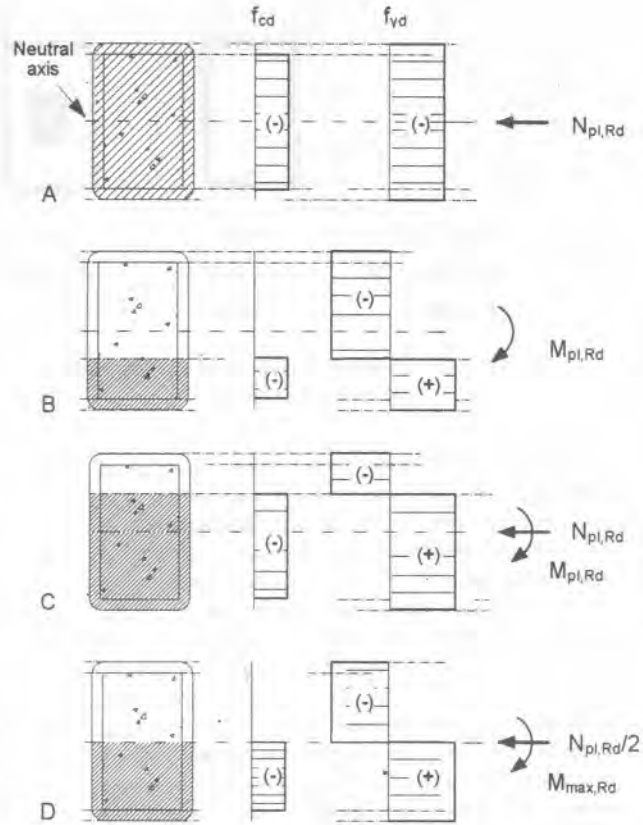


Figure 4 Development of stress blocks at different points on the interaction diagram

**Shortcomings of EBCS 4 1995 Design Procedure**

One of the reasons for the limited applicability of CFTs is attributed to the amount of computational effort that is involved in the design process while the final results are still approximations to the expected results. Designing CFT cross-section under axial compression and uniaxial moment using the EBCS 4 has, therefore, the following major drawbacks:

- Drawing charts is a necessary and an unavoidable process which is time consuming and computationally demanding.
- The design procedure is of trial-and-error nature by which one needs to draw an interaction curve for each trial section.
- The result is approximate since the curves are constructed from only a limited number of interpolation points.

- It is not easy to calculate the plastic moment capacity as it needs computation of corresponding neutral axis position every time.

The procedure to be proposed in this work alleviates the above-noted shortcomings of the conventional code-based practice and this will be presented in the following section.

**CHART DEVELOPMENT**

**Calculation Method and Scope**

The structural engineering practice calls for a variety of cross-sectional types to be used as compression members and as beam-columns. While the procedure to be proposed in this work is general and may easily be modified for adaptation to a variety of column shapes, the cross-sections considered are those that fulfill the criteria for simplified method of analysis given in the Codes [7, 8].

From the permissible steel ratios  $\omega$  stipulated in the Code Standard [7], those for which  $\omega \leq 4.0$  have been selected for drawing the chart as this range utilizes less amount of steel thus resulting in more economical sections compared to those with higher steel ratios.

For the purpose of this work, the more frequently-used sections – rectangular and square ones – have been studied; however, the procedure to be proposed may easily be used to establish similar charts for other cross sectional shapes.

Applicable structural steel grades have been recommended by the national code standard [7]. For the purpose of this paper, Steel Grade Fe360 with element cross-sectional thicknesses of up to 40mm have been selected. The Code also allows the use of Concrete Grade up to C 60. Nevertheless, in view of the practical considerations of quality of concrete currently attainable in the local construction industry, Concrete Grade of C 30 has been used in this paper for establishing the interaction diagrams. On the other hand, the procedure for establishing improved interaction charts and diagrams are fairly general and can, thus, be used to deal with other grades of steel and concrete.

**Interaction Charts for Axial Compression and Uniaxial Bending**

*Fundamental equations*

Interaction charts are drawn using the stress blocks that show the plastic section capacity of composite sections. The fundamental equations to be used for the development of these charts are given below with respect to typical composite cross-section as shown in Fig. 5.

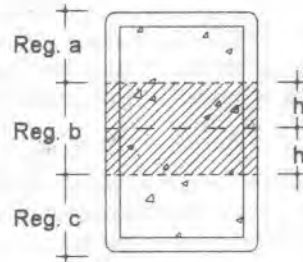


Figure 5 Regions of composite cross-section for computing section capacity

Steel ratio:

$$\omega = \frac{A_s f_{yd}}{A_c f_{cd}} \tag{5}$$

Moment capacity:

$$M_u = (W_{pa} - W_{pan}) f_{yd} + (W_{pc} - W_{pcn}) \frac{f_{cd}}{2} \tag{6}$$

Axial capacity:

$$N_u = A_{sc} f_{cd} + A_{s,net} f_{yd} \tag{7}$$

where:

- $A_s$  and  $A_c$  total cross-sectional area of the steel and concrete sections, respectively.
- $W_{pa}$  and  $W_{pc}$  plastic section modulus of the total steel and concrete section parts, respectively.
- $W_{pan}$  and  $W_{pcn}$  plastic section moduli of the steel and concrete sections within the shaded region (Region b, see Fig. 5), respectively.
- $A_{sc}$  and  $A_{cc}$  cross-sectional areas of the portion of the steel and concrete sections in compression, respectively.

$A_{st}$  cross-sectional area of the portion of the steel section that is subjected to tension

$$A_{s,net} = A_{sc} - A_{st}$$

**Computing section capacity for a given neutral axis**

The determination of the cross-sectional capacity entails two very basic outcomes – proportioning the composite cross-section for a given set of loads (the so-called *design* operation) on one hand and verification of the adequacy of any proposed composite cross-section under a given set of loads (usually referred to as *design checking*). These two points will now be elaborated since the improved procedure to be proposed in this paper address these points.

To this end, certain geometric properties will be used in order to form a non-dimensional parameter to create relationships between the amount of steel and concrete to be used. Thus, the following relationship will be adapted in establishing the interaction curves:

$$x = \frac{b}{l} \quad y = \frac{h}{b} \quad (8)$$

It can also be seen that the following relationships hold for a general rectangular (and square) sections –  $A_c = b'h'$  where  $b' = b - 2t$ ,  $h' = h - 2t$  and  $A_s = bh - A_c$

*Determining value of x for a particular steel ratio  $\omega$*

From Eq. (5), one gets:

$$A_s f_{yd} = \omega A_c f_{cd} \quad (9)$$

In Eq. (9), for a given steel ratio and material condition, the only unknown is the variable quantity  $x$  as given by Eq. (8). Thus, one can explicitly solve for  $x$  as follows after a series of substitutions and re-arrangement:

$$x = \frac{(f_{yd} + \omega f_{cd})(1+y) + \sqrt{(f_{yd} + \omega f_{cd})(1+y))^2 - 4\omega f_{cd}(\omega \alpha_s y + f_{yd})}}{\omega f_{cd} y} \quad (10a)$$

For square section ( where  $y = 1$  ).

$$x = \frac{2(f_{yd} + \omega f_{cd}) + \sqrt{2(f_{yd} + \omega f_{cd})^2 - 4\omega f_{cd}(\omega \alpha_s + f_{yd})}}{\omega f_{cd}} \quad (10b)$$

This is a very important relationship for proportioning the material content of a composite column when the steel ratio  $\omega$  is established a priori.

*Moment and axial load capacities for various neutral axis positions*

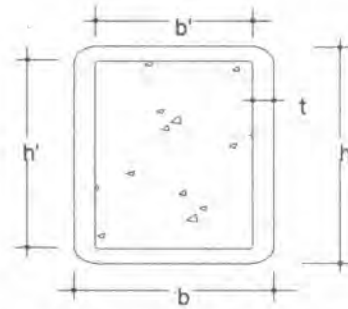


Figure 6 Notations and dimensions

Moment and axial-load capacities can be computed from assumed neutral axis positions. Each position of the neutral axis represents one point on the interaction curve for section capacity. Sufficiently large number of points need be processed to obtain a smooth curve that represents the capacity of a given cross-section. On the other hand, use of equations to generate the interaction curves will avail more refined charts that will eliminate the inherent drawbacks of using the four-point curve approximation stipulated in EBCS 4 [7].

The use of non-dimensional parameters  $\nu$  and  $\mu$ , rather than the corresponding dimensioned variables  $N$  and  $M$ , facilitates the construction and implementation of force-moment interaction diagrams. To this end, expressions for axial forces  $\nu$  are normalized by dividing through  $A_c f_{cd}$ . Similarly, expressions for normalized flexural moments  $\mu$  are obtained by dividing corresponding terms with  $A_c f_{cd} h'$ . Thus, the normalized axial force parameter  $\nu$  and the normalized flexural moment term  $\mu$  for a rectangular (and square) sections are obtained from:

$$\nu = \frac{N_u}{A_c f_{cd}} \quad (11a)$$

$$\mu = \frac{M_u}{A_c f_{cd} h'} \quad (11b)$$

These equations will be used subsequently to establish the interaction diagram for concrete-filled rectangular

and square steel tubes. Details for the determination of  $N$  and  $M$  for the implementation of Eqs. (11) will be presented. Those equations will then be used to establish  $\nu$  and  $\mu$  in terms of cross-sectional and material properties of the composite sections under consideration and, afterwards, to produce the improved uniaxial-bending interaction diagrams.

To establish the desired relationships, four different cases of neutral axis position are selected. The position of the neutral axis varies depending on the relative size of the bending moment and the associate axial force. These cases will be dealt with separately.

Case i: When the whole cross section is under compression

1. Moment Capacity

Since the whole part is in compression the moment capacity requirements becomes zero. The capacity of the cross-section will be fully utilized to resist the direct axial compression; thus,

$$M_u = 0 \tag{12a}$$

Accordingly, in this particular instance,

$$\mu = 0 \tag{12b}$$

2. Axial load capacity

$$N_u = N_{pl,rd} \tag{12c}$$

where  $N_{pl,rd} = A_c f_{cd} + A_s f_{yd}$

Noting that  $A_c = b'h'$  and  $A_s = bh - A_c$ , one gets:

$$\nu = \frac{A_c f_{cd} + A_s f_{yd}}{A_c f_{cd}} \tag{12d}$$

Substituting appropriate terms and dividing both the numerator and denominator of Eq. (12d) by  $t^2$  and simplifying, one obtains the desired expression for  $\nu = N_u / N_{pl,rd}$  in terms of cross-sectional parameters defined by Eq. (8) and material properties as:

$$\nu = \frac{(x-2)(xy-2)f_{cd} + [x^2y - (x-2)(xy-2)]f_{yd}}{(x-2)(xy-2)f_{cd}} \tag{12e}$$

Case ii. Some portion of the flange of the steel section will be in tension while other parts of the cross-section in compression as shown in Fig. 7. Under this circumstance, therefore, the section will develop both bending moment and axial-force resistance. Thus,

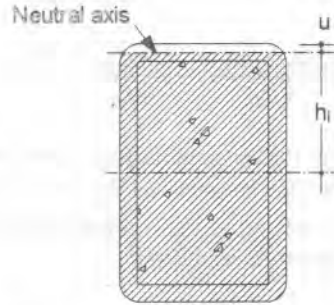


Figure 7 Location of neutral axis for Case (i)

1. Moment Capacity

$$M_u = (W_{pa} - W_{pan}) f_{yd} + (W_{pc} - W_{pcn}) \frac{f_{cd}}{2} \tag{13a}$$

In Eq. (13a), the potential contributions of both steel and concrete sections towards moment capacity are identical. It can be noted that the first term in Eq. (13a) is that portion of moment capacity due to steel while the second one is that due to concrete. Nevertheless, in this case, only the steel portion contributes towards effectively resisting the flexural stress. Thus, Eq. (13a) modifies to:

$$M_u = (W_{pa} - W_{pan}) f_{yd} \tag{13b}$$

Following a similar procedure established in Case (i) above and employing the following relationships -  $W_{pa} = bh^2/4$ ,  $W_{pan} = b(h-2u)^2/4$  where  $u = h/2 - h_1$ , as shown in Fig. 7 - one gets, after a series of substitutions and simplifications, an expression for  $\mu = M_u / A_c f_{cd} h'$  in terms of the cross-sectional parameters and material properties as follows:

$$\mu = \frac{0.25[x^3y^2 - x(xy-2u/t)^2]f_{yd}}{(x-2)(xy-2)^2f_{cd}} \tag{13c}$$

2. Axial load capacity

Noting that  $N_u = N_{pl,Rd} - 2bu f_{yd}$ , one obtains:

$$N_u = A_{cc} f_{cd} + A_{s,net} f_{yd} \quad (13d)$$

Taking the following relationships into account,  $A_c = b'h'$  and  $A_s = bh - b'h'$ , one gets:

$$v = \frac{A_c f_{cd} + A_s f_{yd} - 2bu f_{yd}}{A_c f_{cd}} \quad (13e)$$

which, after further simplification, provides the desired relationship  $v = N_u / N_{pl,Rd}$  in terms of the geometric parameters and material properties as follows:

$$v = \frac{(x-2)(xy-2)f_{cd} + \{x^2y - (x-2)(xy-2)\}f_{yd}}{(x-2)(xy-2)f_{cd}} - \frac{2x(u/t)f_{yd}}{(x-2)(xy-2)f_{cd}} \quad (13f)$$

3. Values of  $\frac{h_i}{t}$  used

Values of  $h_i/t$  used are  $0.5xy+1$ ,  $0.5xy-2/3$  and  $0.5xy-1/3$  where  $x$  and  $y$  are defined as in Eq. (8).

Case iii. When more than half of the cross-sectional area is under compression (Fig. 8)

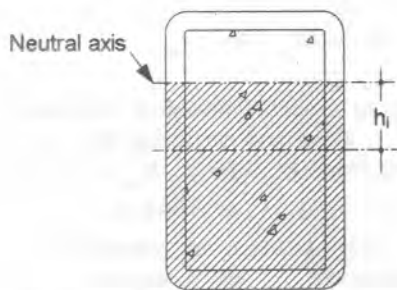


Figure 8 Location of neutral axis for Case (iii)

1. Moment Capacity

In this case, the contribution of both steel and concrete sections will be considered. Thus,

$$M_u = (W_{pa} - W_{pan}) f_{yd} + (W_{pc} - W_{pcn}) \frac{f_{cd}}{2} \quad (14a)$$

Again, taking into account the following relationships:  $W_{pa} = (bh^2 - b'h'^2)/4$ ,

$$W_{pan} = (b-b')h_i^2, \quad W_{pc} = b'h'^2/4,$$

$W_{pcn} = b'h_i^2$ , and employing extensive substitution and simplification, one obtains an expression for  $\mu = M_u / A_c f_{cd} h'$  as follows:

$$\mu = \frac{0.25[x^3y^2 - (x-2)(xy-2)^2 - 2(h_i/t)^2] f_{yd} + [0.25(x-2)(xy-2)^2 - (x-2)(h_i/t)^2] f_{cd}/2}{(x-2)(xy-2)^2 f_{cd}} \quad (14b)$$

2. Axial load capacity

In a similar manner, the relationship between the non-dimensional parameter  $v$  and the cross-sectional as well as material properties becomes:

$$v = \frac{(x-2)(xy/2 - 2 + h_i/t)f_{cd} + 4(h_i/t)f_{yd}}{(x-2)(xy-2)f_{cd}} \quad (14c)$$

3. Values of  $h_i/t$  used

Values of  $h_i/t$  used are 0,  $0.1xy$ ,  $0.2xy$ ,  $0.3xy$  and  $0.4xy$ .

Case iv. When less than half of the cross-sectional area is under compression (Fig. 9)

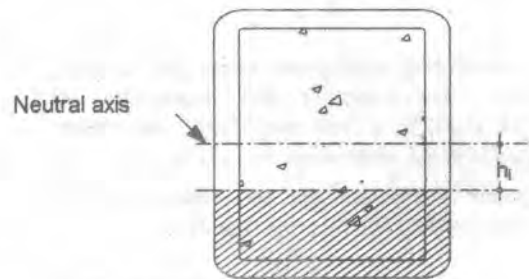


Figure 9 Location of neutral axis for Case (iv)



## 1. Moment Capacity

Moment capacity for this case is equal to that given as in Case (iii) for corresponding neutral axis positions.

## 2. Axial load capacity

The axial load capacity is computed as in Case (iii) using Eq. (14c).

3. Values of  $h/t$  used

Values of  $h/t$  used are 0.1xy, 0.2xy, 0.3xy and 0.4xy.

**Improved Uniaxial Charts**

It is a common practice to develop the so-called interaction charts and diagrams for a variety of reasonably usable cross-sectional dimensions or dimensional ratios. Such charts have been developed

using the improved procedure suggested in this work and proposed for a number of such combinations [10].

For the purpose of this paper, interaction diagrams have been established both for rectangular and square sections and for concrete Grade C 30 and steel Grade Fe 360. Typical improved charts for one case of a rectangular section with height to width ratio  $h/b = 2$  and one for a square cross-section are given, respectively, in Fig. 10 and Fig. 11. It should be understood that these choices of particular material grade or cross-sectional dimensions, especially in the case of the rectangular section, do not create any imitations on the procedure outlines earlier for the production of these charts. The expressions and relationships established are general and, thus, can be implemented for various size proportions and material types provided they meet the provisions of the Code [7] as stipulated earlier in Sec. 3.1 above.

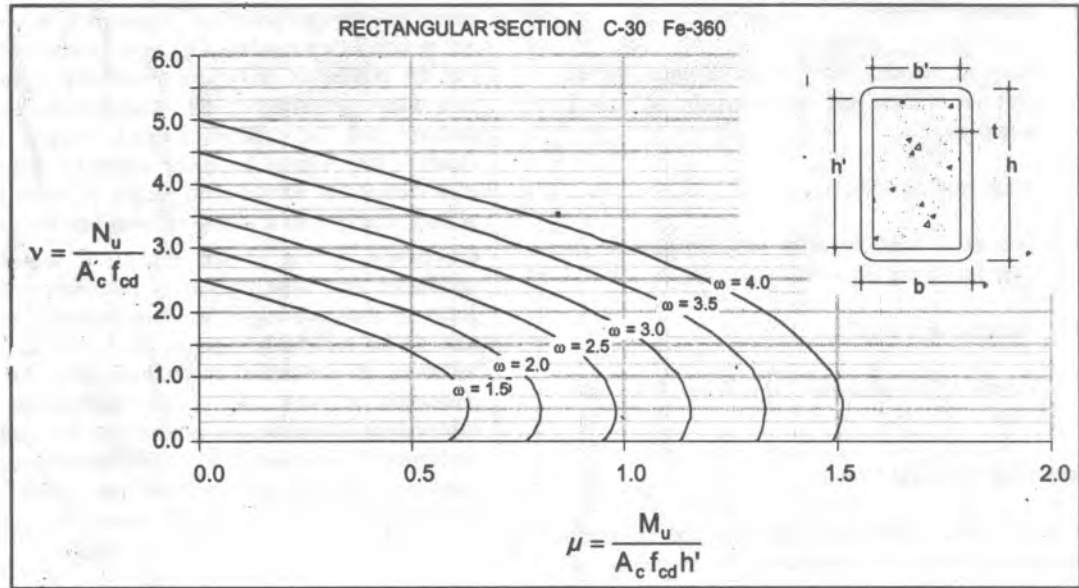


Figure 10 Improved interaction diagram for a rectangular section with  $h/b = 2$

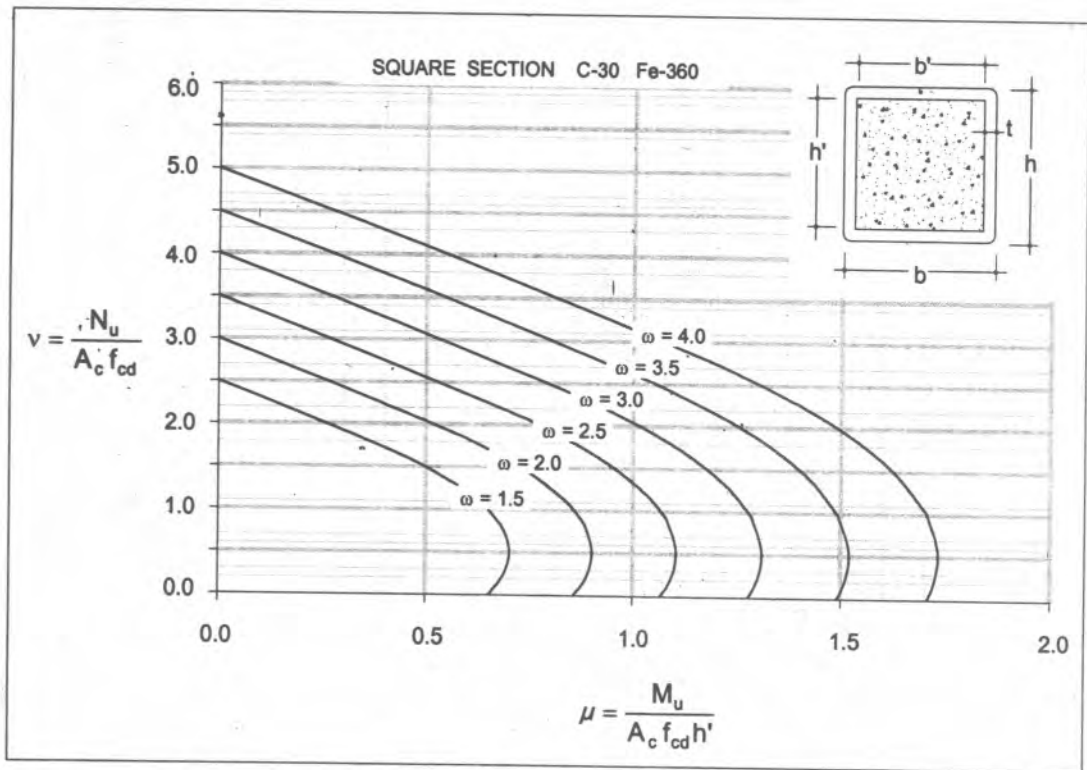


Figure 11 Improved interaction diagram for a square section

NUMERICAL EXAMPLES

Application of the uniaxial interaction diagrams per the proposed improved uniaxial-chart procedure is identical to similar charts although the quality of the results obtained using the improved procedure is superior. The potential capabilities of the proposed charts will be demonstrated through the following examples.

**Example 1:** Design of a square column subjected to uniaxial bending.

Given: Action Effect: Factored loads allowing for initial eccentricity and slenderness effect.

$$N_{sd} = 435.20 \text{ kN} \quad M_{sdx} = 174.08 \text{ kNm}$$

Materials Data: Concrete Grade C 30  
Steel Grade Fe 360

Required: Dimension of cross-section and thickness of steel

Solution: Assume column size, column concrete size,  $b' \times h' = 200\text{mm} \times 200\text{mm}$

$$f_{cd} = \frac{f_{ck}}{\gamma_c} = 16$$

$$A_c f_{cd} = 200 \times 200 \times 16 = 640,000 \text{ N} = 640 \text{ kN}$$

$$\nu = \frac{N_{sd}}{A_c f_{cd}} = \frac{43520}{640} = 0.68 \quad \mu = \frac{M_{sd}}{A_c f_{cd} h'} = \frac{17408}{640 \times 200} = 136$$

Using chart for square section (given with Example 2 below):

$$\omega = 3.15$$

$$\omega = \frac{A_s f_{yd}}{A_c f_{cd}} \rightarrow A_s = \frac{\omega A_c f_{cd}}{f_{yd}} = \frac{3.15 \times 640,000}{213.64} = 9,436.6 \text{ mm}^2$$

$$A_s + A_c = 200^2 + 9,437 = 49,437 \text{ mm}^2$$

$$b = h = \sqrt{49,437} = 222.34 \text{ mm}$$

$$t = 0.5 \times (222.34 - 200) = 11.17 \text{ mm}$$

Thus, use  $t = 12\text{mm}$  and square column of overall

dimension  $224\text{mm} \times 224 \text{ mm}$ .

**Example 2:** Verification of the solution of Example 1 using the procedure in EBCS 4.

Given: Overall depth ( $d$ ) = 224 mm

Thickness of steel section  $t = 12 \text{ mm}$

Action Effect: Factored loads allowing for initial eccentricity and slenderness effect

$$N_{sd} = 435.2 \text{ kN}$$

$$M_{sdx} = 174.08 \text{ kNm}$$

Materials Data: Concrete Grade C30  
Steel Grade Fe360

Required: To verify the adequacy of the section for the given loading using the procedure in EBCS 4-1995.

Solution: To draw the interaction curve according to the provisions of EBCS 4, the following section capacities are determined:

- Plastic resistance to compression load

$$N_{pl,Rd} = A_c f_{cd} + A_s f_{yd} = 200 \times 200 \times 16 + (224 \times 224 - 200 \times 200) \times 213.64 = 2814 \text{ kN}$$

- Compressive resistance of the concrete part

$$N_{pm,Rd} = A_c f_{cd} = 200 \times 200 \times 16 \times 10^{-3} = 640 \text{ kN}$$

- Neutral axis position for zero axial compression ( $h_n$ )

From Fig. E1 for zero axial force:

$$F_{cc} = F_{st} \tag{a}$$

$$F_{cc} = (100 - h_n) \times 200 \times 16$$

$$F_{st} = 2 \times 12 \times 2h_n \times 213.64$$

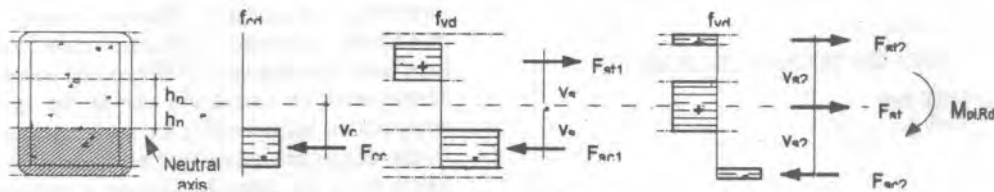


Figure E1 Stress block for zero axial compressive force

Substituting the above equations into Eq. (a) and solving for  $h_n$

$$h_n = 23.8 \text{ mm}$$

- Plastic moment capacity for zero axial force,  $M_{pl,rd}$

Using the value of the neutral axis depth computed above:

$$M_{pl,rd} = F_{cc} y_c + 2F_{sc1} y_{s1} + 2F_{sc2} y_{s2} \quad (b)$$

$$F_{cc} = (100 - h_n) \times 200 \times 16 \times 10^{-3} = 243 \text{ kN}$$

$$y_c = 61.9 \text{ mm}$$

$$F_{sc1} = 2 \times 12 \times (100 - 23.8) \times 213.64 = 390.8 \text{ kN}$$

$$y_{s1} = 61.89 \text{ mm}$$

$$F_{sc2} = 224 \times 12 \times 213.64 = 574.26 \text{ kN}$$

$$y_{s2} = 112 \text{ mm}$$

Substituting the above values into Eq. (b) above, one gets:

$$M_{pl,rd} = 192.05 \text{ kN-m}$$

- Maximum moment capacity,  $M_{max,rd}$

Maximum moment capacity occurs when the neutral axis passes through the centroid. The corresponding stress block is shown in Fig. E2.

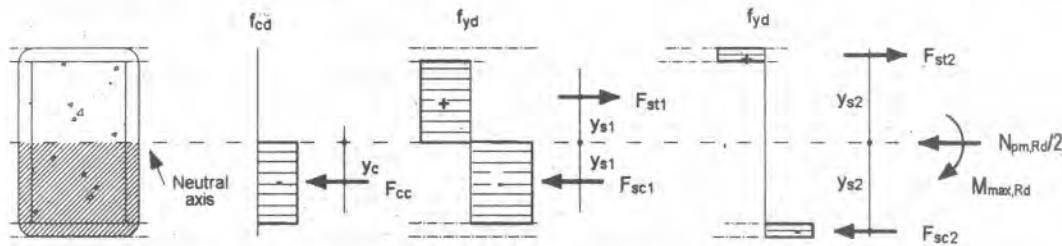


Figure E2 Stress block for maximum moment

$$M_{max,rd} = F_{cc} y_c + 2F_{sc1} y_{s1} + 2F_{sc2} y_{s2} \quad (c)$$

$$F_{cc} = 100 \times 200 \times 16 = 320 \text{ kN}$$

$$y_c = 50 \text{ mm}$$

$$F_{sc1} = 2 \times 12 \times 100 \times 213.64 = 512.7 \text{ kN}$$

$$y_{s1} = 50 \text{ mm}$$

$$F_{sc2} = 224 \times 12 \times 213.64 = 574.26 \text{ kN}$$

$$y_{s2} = 112 \text{ mm}$$

Substituting the above values into Eq. (c) above,

$$M_{max,rd} = 195.9 \text{ kNm}$$

The values of the four points for drawing the interaction curve can be computed as follows:

$$\text{Point A: } \mu = 0 \quad \nu = 1$$

$$\text{Point B: } \mu = 1 \quad \nu = 0$$

$$\text{Point C: } \mu = 1 \quad \nu = \frac{N_{pm,rd}}{N_{pl,rd}} = \frac{640}{2814} = 0.23$$

$$\text{Point D: } \mu = \frac{M_{max,rd}}{M_{pl,rd}} = \frac{195.9}{192.05} = 1.02$$

$$\nu = \frac{0.5N_{pm,rd}}{N_{pl,rd}} = 0.115$$

Using this point, an interaction curve is drawn as shown in Fig. E3.

Point corresponding to the applied load:

$$\mu_{sd} = \frac{M_{sd}}{M_{pl,rd}} = 0.91 \quad \nu_{sd} = \frac{N_{sd}}{N_{pl,rd}} = 0.15$$

This point lies within the interaction curve as shown in Fig. E3. Thus, the section is sufficient.

## CONCLUSION

Concrete-filled steel tubes used as structural columns have significant economic, structural and functional advantages. However, their design procedures stipulated in various code standards have been computationally demanding as they need development of interaction curves for each trial cross-section considered in the design process. That is, the design procedure that has been proposed in EBCS 4 [7], for example, follows a trial-and-error

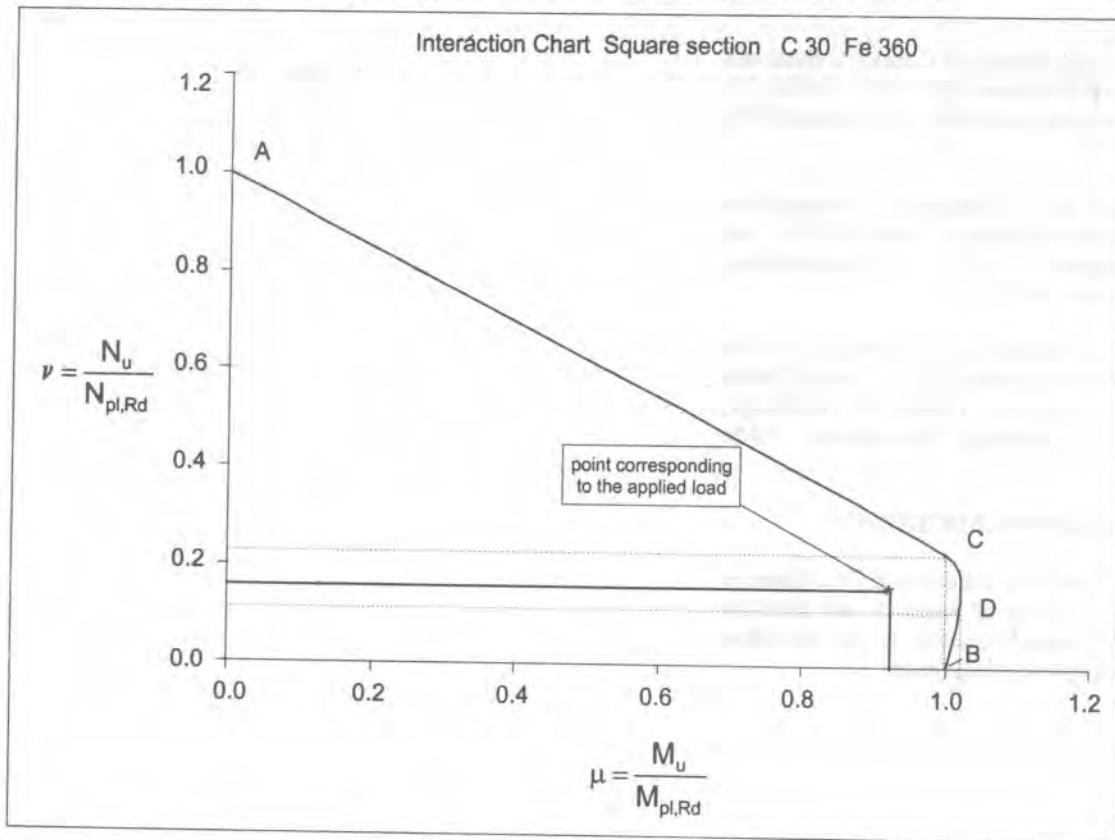


Figure E3 Normalized interaction curve for Example 2

approach to determine the necessary cross-section for a given load.

To alleviate this problem, normalized charts have been produced that simplify the design calculation. The charts can be used to directly compute the amount of steel required for a given cross-section without resorting to the code-based trial-and-error procedure. Besides being computationally efficient, the produced charts also provide more accurate results than using the method stipulated in EBCS 4.

**REFERENCES**

- [1] Eurocode Course Lecture Note, Structural Steel Work Eurocodes, Development of a Trans-National Approach, Chapter VII – Composite Columns, 2001.
- [2] M. Johansson and K. Gylltoft, Structural Behavior of Slender Circular Steel-Concrete Composite Columns Under Various Means of Load Application, Steel and Composite Structures, Vol. 1, No. 4, Chalmers University of Technology, Sweden, 2001.
- [3] J.F. Hajjar, Concrete-Filled Steel Tube Columns Under Earthquake Loads", Prog. Structural Engineering Material, 2000.
- [4] K. Lahlou, M. Lachemi, and P.C. Aitein, "Confined High Strength Concrete Under Dynamic Compressive Loading", Journal of structural engineering, ASCE, Vol.125, 1999.
- [5] M. Viest et al, "Composite Construction Design for Buildings", ASCE, McGraw-Hill, New York 1997.
- [6] EBCS 2-1995, Part 2: Design Aids for Reinforced Concrete Sections on the basis of EBCS-2: 1995, Ministry of Works & Urban Development, Addis Ababa, 1997.
- [7] EBCS 4 1995, Design of Composite Steel and Concrete Structures, Ministry of Works & Urban Development, Addis Ababa, 1995.

- [8] Eurocode 4: Design of Composite Steel and Concrete Structures: ENV 1994-1-1 Part 1.1: General rules and rules for buildings, CEN, 2002.
- [9] H. Bode and R. Bergmann, *Betongefüllte Stahlhohlprofilstützen*, Markblatt 167 der Beratungsstelle für Stahlverwendung, Düsseldorf, 1985.
- [10] Ermiyas Ketema, 2005, *Design Aid for Composite Column*, M.Sc. Thesis, Addis Ababa University, Faculty of Technology, Civil Engineering Department, Addis Ababa.

#### **ACKNOWLEDGEMENT**

The authors gratefully acknowledge the financial support of the Office of Research and Graduate Office, Addis Ababa University, to the first author during the preparation of this paper.